Noise Enhancement due to Quantum Coherence in Coupled Quantum Dots

G. Kießlich,[1,2] E. Schöll,[2] T. Brandes,[2] F. Hohls,[3] and R. J. Haug[3]

[1]*School of Physics and Astronomy, University of Nottingham, Nottingham NG7 2RD, United Kingdom*
[2]*Institut für Theoretische Physik, Technische Universität Berlin, D-10623 Berlin, Germany*
[3]*Institut für Festkörperphysik, Leibniz Universität Hannover, D-30167 Hannover, Germany*
(Received 12 June 2007; published 16 November 2007)

We show that the intriguing observation of noise enhancement in the charge transport through two vertically coupled quantum dots can be explained by the interplay of quantum coherence and strong Coulomb blockade. We demonstrate that this novel mechanism for super-Poissonian charge transfer is very sensitive to decoherence caused by electron-phonon scattering as inferred from the measured temperature dependence.

The direct manifestation of quantum coherence in time-averaged transport observables of nanoscale conductors such as current or low-frequency current fluctuations is of great benefit since it allows for the study of decoherence in a straightforward manner. Quantum dots (QDs) coupled in series provide a perfect system to explore such effects since the quantum superposition of states in different dots has an immediate influence on the charge transfer [1]. The effect of quantum coherence has been experimentally addressed mostly with respect to the average or time-dependent currents (e.g., in Ref. [2]), whereas until now current fluctuations as a very sensitive diagnostic tool [3–5] have not been investigated for this purpose.

In this Letter we demonstrate that our recent low-frequency shot noise data provide such a tool and are in fact a direct indicator of quantum coherent coupling between two layers of self-assembled InAs QDs [6]. In our device, QD stacks are formed such that vertical tunneling through three barriers becomes possible. The corresponding current vs applied bias voltage exhibits sharp peaks caused by the alignment of levels in a single QD stack. At the edges of these resonances the noise is enhanced above the Poissonian value for uncorrelated electron transfer $2e\langle I \rangle$ (e is the unit charge and $\langle I \rangle$ is the average current).

We find a striking agreement between our data and our calculations of this novel mechanism based on a quantum master equation for super-Poissonian charge transport in a single QD stack, which shows that contrary to the common view capacitive coupling between the stacks is not needed to explain the observed features. Typically, such noise behavior is associated with electron bunching in the charge transfer and has therefore received remarkable interest in recent experimental [7–11] and theoretical work [12–17]. We also show that the decoherence due to electron-phonon scattering causes a temperature dependence that agrees with the measurements, allowing us to clearly identify the crossover between coherent and sequential tunneling.

Experiment.—Here we summarize the relevant features of the device and the experimental data [6]. The InAs quantum dot stacks are prepared by Stranski-Krastanov growth on AlAs and are sandwiched between three AlAs tunneling barriers. The three-dimensional electron reservoirs on both sides are formed in graded doped GaAs. The pyramid-shaped quantum dots partially penetrate the middle and top barrier which results in asymmetric tunneling rates. A sketch of the device geometry is shown in Fig. 1 (left). For the considered direction of the current the emitter barrier is effectively thinner, $\Gamma_e > \Gamma_c$. The leverage factors for the quantum dots QD1 and QD2, i.e., the ratios of the potential drop between emitter and dot to the applied voltage V_{SD}, are estimated from the device geometry: $\eta_1 \approx 0.25$ and $\eta_2 \approx 0.55$, respectively. The Fermi energy in the reservoir can be determined from a comparison with magnetotunneling experiments for devices with only one layer of quantum dots. For devices with an otherwise identical growth scheme one finds an emitter Fermi level $\mu_e \approx 13.6$ meV [18].
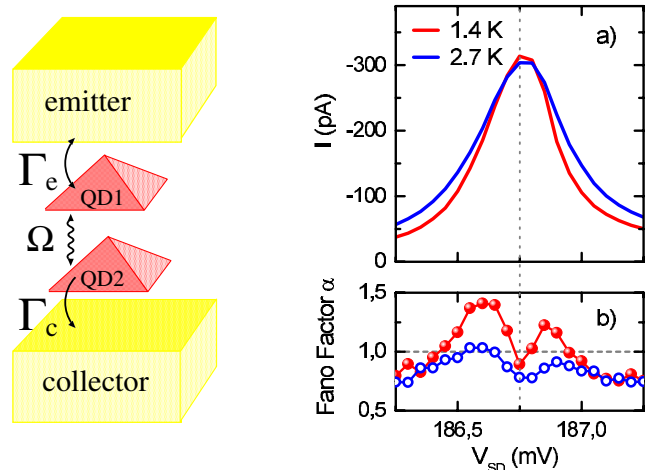

FIG. 1 (color online). Left: Sketch of a quantum dot stack with contact regions, contact couplings Γ_e, Γ_c and the tunnel matrix element Ω for coupling between the dots. The electrons tunnel from the top (emitter) reservoir via the dots into the bottom (collector) reservoir. Right: (a) Measured current and (b) Fano factor vs bias voltage.

206602-1

Because of the small size of the InAs quantum dots on AlAs the ground state energies ε_1 and ε_2 both lie above the Fermi energy μ_e and no current can flow through the device for $V_{SD} = 0$. Because of the growth condition we also find that the top quantum dot QD1 is larger than the bottom one, $\varepsilon_1 < \varepsilon_2$. By applying a finite voltage $V_{SD} > 0$ the energy levels $\varepsilon_i(V_{SD})$ of the dots are shifted downwards by $e\eta_i V_{SD}$ and brought into resonance. For $\mu_e > \varepsilon_1 = \varepsilon_2 > 0$ we observe a peak in the tunneling current [Fig. 1(a)] [19]. With increasing temperature the resonance broadens while the maximum remains nearly constant. Also a slight asymmetry with respect to the maximum can be observed. Both facts provide some indication for electron-phonon scattering in the tunneling process [20,21] which will be discussed below in more detail.

The noise properties of the current in the range of the resonant tunneling peak are shown in Fig. 1(b). The Fano factor $\alpha = S(0)/(2e\langle I\rangle)$ ($S(0)$ is the zero-frequency noise) vs bias voltage displays an asymmetric double-peak structure with the maxima at the edges of the current resonance and $\alpha > 1$ indicating super-Poissonian noise. The noise is more sensitive to the temperature than the current: for larger temperatures the Fano factor peaks become smaller, and the super-Poissonian behavior vanishes. Far from the resonance we observe $\alpha < 1$ which we assume is due to some background current signal originated from leakage channels. In an ideal device the off-resonance electron transfer is Poissonian.

Model.—We consider the coupled QD system as sketched in Fig. 1 (left) in the strong Coulomb blockade regime; i.e., only the occupation by a single excess electron is allowed. This restricts the dimension of the Hilbert space of the dot system spanned by the basis states $|0\rangle \equiv |N, M\rangle$ for no excess electrons, $|1\rangle \equiv |N + 1, M\rangle$ for one excess electron in QD1, and $|2\rangle \equiv |N, M + 1\rangle$ for one excess electron in QD2. The corresponding Hamiltonian can be written as

$$H_D = \frac{\varepsilon}{2}\sigma_z + \Omega\sigma_x + \frac{1}{2}\sigma_z\hat{A} + H_B,$$
$$\hat{A} = \sum_Q g_Q(a_{-Q} + a_Q^\dagger), \qquad H_B = \sum_Q \omega_Q a_Q^\dagger a_Q, \tag{1}$$

with the detuning of the QD levels $\varepsilon \equiv \varepsilon_1 - \varepsilon_2$ which corresponds to an applied bias voltage, the tunnel coupling between the dots Ω (see Fig. 1), $\sigma_z = |1\rangle\langle1| - |2\rangle\langle2|$, and $\sigma_x = |1\rangle\langle2| + |2\rangle\langle1|$. The second part in (1) describes the electron-phonon coupling and the phonon bath where $a_Q^\dagger$ is the creation operator of a phonon mode Q with frequency ω_Q and g_Q is the coupling constant of electrons to phonon mode Q (for more details see Ref. [22]). This spin-boson Hamiltonian will be coupled to the external electron reservoirs of emitter and collector contact. The quantum master equation for the reduced density matrix is then obtained from the von Neumann equation for the total density matrix in Born-Markov approximation for weak

contact coupling [23] and second-order perturbation theory in the electron-phonon coupling [22]:

$$\frac{d}{dt}\rho = \begin{pmatrix} -\Gamma_e & 0 & \Gamma_c e^{i\chi} & 0 & 0 \\ \Gamma_e & 0 & 0 & 0 & 2\Omega \\ 0 & 0 & -\Gamma_c & 0 & -2\Omega \\ 0 & \gamma_+ & -\gamma_- & -\frac{\Gamma_c}{2} - \gamma & -\varepsilon \\ 0 & -\Omega & \Omega & \varepsilon & -\frac{\Gamma_c}{2} - \gamma \end{pmatrix}\rho \tag{2}$$

with the reduced density matrix in vector form $\rho = (\rho_{00}, \rho_{11}, \rho_{22}, \mathrm{Re}[\rho_{12}], \mathrm{Im}[\rho_{12}])^T$ and the rates for coupling to the emitter or collector contact $\Gamma_{e/c}$, respectively, (see Fig. 1 left) [24]. The counting field $e^{i\chi}$ which will be needed to calculate the current and the noise (see below) enters the matrix element in (2), where an electron jumps into the collector [25].

The rates for the electron-phonon interaction in Eq. (2) are [22,26]

$$\gamma = \frac{g\pi}{\Delta^2}\left[\frac{\varepsilon^2}{\beta} + 2\Omega^2\Delta e^{-\Delta/\omega_c}\coth\left(\frac{\beta\Delta}{2}\right)\right]$$
$$\gamma_\pm = g\frac{\pi\Omega}{\Delta^2}\left[\frac{\varepsilon}{\beta} - \frac{\varepsilon}{2}\Delta e^{-\Delta/\omega_c}\coth\left(\frac{\beta\Delta}{2}\right) \mp \frac{\Delta^2}{2}e^{-\Delta/\omega_c}\right] \tag{3}$$

with a dimensionless coupling constant g, a high-frequency cutoff ω_c being an effective Debye frequency, $\Delta = \sqrt{\varepsilon^2 + 4\Omega^2}$ and $\beta = (k_B T)^{-1}$. These rates were derived for a bosonic environment with Ohmic spectral density $\rho(\omega) = g\omega e^{-\omega/\omega_c}\Theta(\omega)$ which corresponds to bulk piezoelectric phonons in the limit $\omega_c \to \infty$ and vanishing longitudinal speed of sound. Here and in the following we neglect the imaginary parts of $\gamma_\pm$.

The average current and the noise is computed with the help of the cumulant generating function $F(\chi)$. It is defined by $\exp[-F(\chi)] = \sum_N P(N, t_0)\exp[iN\chi]$ with the distribution function $P(N, t_0)$ of the number N of transferred charges in the time interval t_0. We obtain $F(\chi)$ as the eigenvalue of the transition matrix in Eq. (2) which approaches zero for $\chi = 0$ [25]. From the cumulant generating function the cumulants $C_k = -(-i\partial_\chi)^k F(\chi)|_{\chi=0}$ are obtained. Then, the average current is $\langle I\rangle = eC_1$, the zero-frequency noise is $S(0) = 2e^2 C_2$, and the Fano factor reads $\alpha = C_2/C_1$. It is smaller than unity for sub-Poissonian and larger than unity for super-Poissonian charge transfer.

Discussion.—Without electron-phonon interaction ($\gamma = \gamma_\pm = 0$) we reproduce the known results for the current $\langle I\rangle = e4\Gamma_e\Gamma_c\Omega^2/[4\Omega^2(2\Gamma_e + \Gamma_c) + \Gamma_e\Gamma_c^2 + 4\varepsilon^2\Gamma_e]$ [27,28] which provides a Lorentzian with respect to the detuning (bias voltage) ε as shown by the dotted curve in Fig. 2(a) and the Fano factor [23,26]

$$\alpha = 1 - 8\Gamma_e\Omega^2\frac{4\varepsilon^2(\Gamma_c - \Gamma_e) + 3\Gamma_e\Gamma_c^2 + \Gamma_c^3 + 8\Gamma_c\Omega^2}{[\Gamma_e\Gamma_c^2 + 4\Gamma_e\varepsilon^2 + 4\Omega^2(\Gamma_c + 2\Gamma_e)]^2}. \tag{4}$$
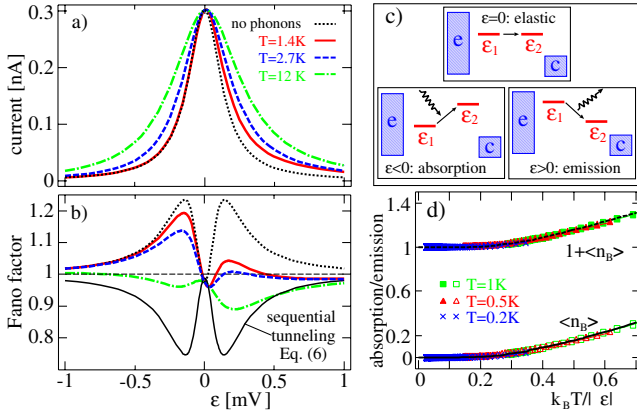
FIG. 2 (color online).   Theory: (a) Current, (b) Fano factor vs
level detuning $\varepsilon = \varepsilon_1 - \varepsilon_2$ (bias voltage) for strong Coulomb
blockade (only one electron in the dot system). (c) Band schemes
for tunneling through the dot system in different bias situations.
(d) absorption and emission rates normalized by the spontaneous
emission rate vs $k_B T/|\varepsilon|$. The lower curve indicates the Bose-
Einstein distribution $\langle n_B \rangle$, whereas the upper curve shows $\langle n_B \rangle +$
1. Parameters: $\Gamma_e = 0.1$ meV, $\Gamma_c = 2.5$ μeV, $\Omega = 0.1$ meV,
$g = 8 \times 10^{-4}$, $\omega_c = 5$ meV.

Super-Poissonian charge transfer occurs when the second
term in (4) becomes negative. This is fulfilled for $\varepsilon \neq 0$
and $\Gamma_c < \Gamma_e$. In this case, the Coulomb interaction is more
effective due to the smaller collector coupling, and two
Fano factor peaks larger than unity and symmetric with
respect to the current maximum appear [see dotted curve in
Fig. 2(b)]. This bunching effect can be understood in the
basis of the bonding and antibonding state by the asym-
metry of their contact couplings similar to the dynamical
channel blockade [12,14]. We emphasize that this super-
Poissonian transport behavior is only obtained for
(i) coherent coupling between the dots and for (ii) strong
Coulomb blockade. In order to verify this, we address these
two issues in more detail. (i) Consider a sequential tunnel-
ing approach, i.e., without nondiagonal elements of the
density matrix: The master equation in strong Coulomb
blockade for the diagonal elements of the density matrix
$\tilde{\rho} = (\rho_{00}, \rho_{11}, \rho_{22})^T$ reads

$$\frac{d}{dt}\tilde{\rho} = \begin{pmatrix} -\Gamma_e & 0 & \Gamma_c e^{i\chi} \\ \Gamma_e & -Z & Z \\ 0 & Z & -(\Gamma_c + Z) \end{pmatrix} \tilde{\rho}, \qquad (5)$$

where $Z \equiv \frac{4\Omega^2}{\Gamma_c}[1 + (2\varepsilon/\Gamma_c)^2]^{-1}$ is Fermi's golden rule
transition rate between states $|1\rangle$ and $|2\rangle$ [29]. Note that
due to the Coulomb blockade only the collector coupling
enters this rate. Current and noise are computed by means
of the cumulant generating function. Then this approach
yields the same expression for the current as the coherent
description (2). The Fano factor is

$$\alpha = 1 - \frac{4\Omega^2 \Gamma_e (2\Gamma_c + \Gamma_e)(4\varepsilon^2 + \Gamma_c^2) + 32\Gamma_c \Gamma_e \Omega^4}{[\Gamma_e \Gamma_c^2 + 4\Gamma_e \varepsilon^2 + 4\Omega^2(\Gamma_c + 2\Gamma_e)]^2}.$$
$$(6)$$

Clearly, sequential tunneling turns out to be solely sub-
Poissonian since the second term in (6) is always positive.
(ii) In order to relax the constraint of strong Coulomb
blockade we extend the Hilbert space by the basis state
$|3\rangle \equiv |N + 1, M + 1\rangle$ for two excess electrons in the sys-
tem. This leads to a master equation analogous to Eq. (2)
and the resulting Fano factor also indicates overall sub-
Poissonian transport behavior as we have checked numeri-
cally. Thus, to observe the super-Poissonian transport sce-
nario the Coulomb interaction between the dots has to be
larger than the difference of μ_e and the energy where both
single particle dot states are in resonance. Furthermore we
can exclude double occupation of one of the dots since it
has a rather low probability due to the large on site
Coulomb energy in InAs QDs ($U \sim 20$ meV $\gg \mu_e$).

We will now discuss the influence of the finite tempera-
ture: With $k_B T \ll U$ we can assume $f_e(\varepsilon) = 1$ and
$f_c(\varepsilon) = 0$ for the Fermi functions of the leads for a typical
situation as sketched in Fig. 2(c). Therefore temperature
acts solely due to the coupling to the phonon bath.

With electron-phonon interaction the calculated current
and Fano factor vs. level detuning ε are shown in Fig. 2(a)
and 2(b) for three different temperatures. With increasing
temperature the current resonance becomes asymmetri-
cally broadened, whereas the maximum is not affected.
For $\varepsilon < 0$ phonon absorption and for $\varepsilon > 0$ phonon emis-
sion take place; see Fig. 2(c). From the data for the com-
puted current we extract the corresponding phonon
absorption and emission rates normalized by the rate for
spontaneous phonon emission $A(\varepsilon)$: $W_a(\varepsilon)/A(-\varepsilon)$ for $\varepsilon <$
0 and $W_e(\varepsilon)/A(\varepsilon)$ for $\varepsilon < 0$, respectively. According to the
Einstein relations they should equal the Bose-Einstein
distribution $\langle n_B \rangle$ for absorption and $\langle n_B \rangle + 1$ for emission.
In Fig. 2(d) we compare them as a function of $k_B T/|\varepsilon|$
[20].

The double peaks in the Fano factor discussed above,
which were symmetric without coupling to the phonon
bath [dotted curve in Fig. 2(b)], now become asymmetric
with lower values above the resonance. For higher tem-
peratures the Fano factor peaks decrease. This is in com-
plete agreement with our experimental data (Fig. 1). This
demonstrates that in the experiment, the transport of elec-
trons through the dot system can be assumed to be partially
coherent, strongly indicating electron-phonon scattering as
the dephasing mechanism.

It is worth noting that the presented transport behavior
persists over a wide range of Ω as long as $\Gamma_c \ll \Gamma_e, \Omega$.

Furthermore, the low-frequency noise behavior enables
the clear identification of a sequential and a coherent
tunneling regime. In contrast to small temperatures, for
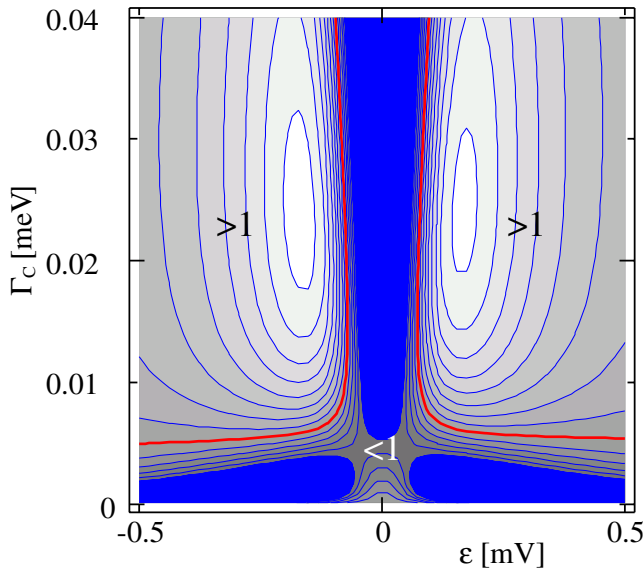higher $T = 12$ K [dash-dotted curve in Fig. 2(b)] the Fano

FIG. 3 (color online). Theory: Fano factor vs level detuning $\varepsilon = \varepsilon_1 - \varepsilon_2$ (bias voltage) and collector coupling Γ_c. The minimum (maximum) Fano factor is 0.9 (1.18), respectively. Contour line spacing is 0.02. Red curves and blue shaded regions correspond to $\alpha = 1$ and $\alpha < 0.9$, respectively, ($T = 12$ K, other parameters are the same as in Fig. 2).

factor indicates sub-Poissonian electron transfer for all bias voltages. Moreover, the Fano factor peaks at the edges of the resonance in the coherent tunneling regime turn into minima. Such behavior is also found by our Fano factor expression for sequential tunneling (6). A corresponding curve is shown in Fig. 2(b) clearly revealing the double minimum feature. Hence a double peak in the Fano factor refers to a coherent tunneling regime, whereas a double minimum indicates a sequential tunneling regime.

The crossover between these two regimes can also be induced by varying the collector coupling Γ_c for fixed couplings Γ_e, Ω and temperature T as shown in Fig. 3. The two different transport regimes are clearly distinguished: For small coupling ($\Gamma_c < 5 \ \mu$eV) the sequential tunneling regime is recognized by the double minima with suppressed noise. For increasing Γ_c a Fano factor larger than unity for $\varepsilon \neq 0$ indicates positive correlations in the charge transfer and consequently refers to coherent tunneling. Here the increased Γ_c leads to shorter dwell time of the electrons on the dot and thus a smaller probability of a phonon absorption as the bath temperature is kept constant. If we increase Γ_c above Γ_e we find again a Fano factor smaller than unity. Therefore the super-Poissonian behavior is most pronounced with a maximum Fano factor for a certain collector coupling.

Conclusions.—We have demonstrated that electron shot noise measurements provide a tool to detect the coherent coupling between quantum dots. We have compared low-frequency noise data with calculations based on quantum master equations which clearly demonstrate that the observed enhancement of the low-frequency noise at low temperatures is caused by the combined effect of strong Coulomb blockade and the quantum coherent transfer of electrons between the dots. We have furthermore shown that electron-phonon scattering as a source of decoherence is responsible for the experimental temperature dependence of current and noise.

[1] W. G. van der Wiel *et al.*, Rev. Mod. Phys. **75,** 1 (2002).
[2] T. Hayashi *et al.*, Phys. Rev. Lett. **91,** 226804 (2003).
[3] Y. M. Blanter and M. Büttiker, Phys. Rep. **336,** 1 (2000).
[4] R. Aguado and T. Brandes, Phys. Rev. Lett. **92,** 206601 (2004).
[5] T. Fujisawa *et al.*, Science **312,** 1634 (2006).
[6] P. Barthold *et al.*, Phys. Rev. Lett. **96,** 246804 (2006).
[7] G. Iannaccone *et al.*, Phys. Rev. Lett. **80,** 1054 (1998).
[8] V. V. Kuznetsov *et al.*, Phys. Rev. B **58,** R10 159 (1998).
[9] S. S. Safonov *et al.*, Phys. Rev. Lett. **91,** 136801 (2003).
[10] S. Gustavsson *et al.*, Phys. Rev. B **74,** 195305 (2006).
[11] O. Zarchin *et al.*, Phys. Rev. Lett. **98,** 066801 (2007).
[12] G. Kießlich, A. Wacker, and E. Schöll, Phys. Rev. B **68,** 125320 (2003).
[13] A. Thielmann *et al.*, Phys. Rev. B **71,** 045341 (2005).
[14] A. Cottet, W. Belzig, and C. Bruder, Phys. Rev. B **70,** 115315 (2004).
[15] W. Belzig, Phys. Rev. B **71,** 161301(R) (2005).
[16] I. Djuric, B. Dong, and H. L. Cui, Appl. Phys. Lett. **87,** 032105 (2005).
[17] J. Aghassi *et al.*, Phys. Rev. B **73,** 195323 (2006).
[18] I. Hapke-Wurst *et al.*, Phys. Rev. B **62,** 12 621 (2000).
[19] N. van der Vaart *et al.*, Phys. Rev. Lett. **74,** 4702 (1995).
[20] T. Fujisawa *et al.*, Science **282,** 932 (1998).
[21] T. Brandes and B. Kramer, Phys. Rev. Lett. **83,** 3021 (1999).
[22] T. Brandes and T. Vorrath, Phys. Rev. B **66,** 075341 (2002).
[23] B. Elattari and S. A. Gurvitz, Phys. Lett. A **292,** 289 (2002).
[24] In Eq. (2) spin polarized electrons are presumed. However, the consideration of spin degeneracy yields a current and Fano factor which only slightly deviate from the ones presented in Fig. 2.
[25] G. Kießlich *et al.*, Phys. Rev. B **73,** 033312 (2006).
[26] T. Brandes, Phys. Rep. **408,** 315 (2005).
[27] T. H. Stoof and Y. V. Nazarov, Phys. Rev. B **53,** 1050 (1996).
[28] S. A. Gurvitz and Y. S. Prager, Phys. Rev. B **53,** 15 932 (1996).
[29] H. Sprekeler *et al.*, Phys. Rev. B **69,** 125328 (2004).